# 51. IWK

Internationales Wissenschaftliches Kolloquium
International Scientific Colloquium

**PROCEEDINGS** 11-15 September 2006

## FACULTY OF ELECTRICAL ENGINEERING AND INFORMATION SCIENCE

# INFORMATION TECHNOLOGY AND ELECTRICAL ENGINEERING - DEVICES AND SYSTEMS, MATERIALS AND TECHNOLOGIES FOR THE FUTURE

Startseite / Index:
http://www.db-thueringen.de/servlets/DocumentServlet?id=12391

TECHNISCHE UNIVERSITÄT
ILMENAU

**Impressum**

Herausgeber: Der Rektor der Technischen Universität Ilmenau
Univ.-Prof. Dr. rer. nat. habil. Peter Scharff

Redaktion: Referat Marketing und Studentische Angelegenheiten
Andrea Schneider

Fakultät für Elektrotechnik und Informationstechnik
Susanne Jakob
Dipl.-Ing. Helge Drumm

Redaktionsschluss: 07. Juli 2006

Technische Realisierung (CD-Rom-Ausgabe):
Institut für Medientechnik an der TU Ilmenau
Dipl.-Ing. Christian Weigel
Dipl.-Ing. Marco Albrecht
Dipl.-Ing. Helge Drumm

Technische Realisierung (Online-Ausgabe):
Universitätsbibliothek Ilmenau
ilmedia
Postfach 10 05 65
98684 Ilmenau

Verlag:
Verlag ISLE, Betriebsstätte des ISLE e.V.
Werner-von-Siemens-Str. 16
98693 Ilrnenau



ISBN (Druckausgabe): 3-938843-15-2
ISBN (CD-Rom-Ausgabe): 3-938843-16-0

Startseite / Index:
http://www.db-thueringen.de/servlets/DocumentServlet?id=12391

51st Internationales Wissenschaftliches Kolloquium
Technische Universität Ilmenau
September 11 – 15, 2006

M. Mihov / K. Brandisky / E. Ratz / P. Mihaylova

# Numerical and experimental investigation of the equivalent circuit parameters of induction machine

## I. INTRODUCTION

During the last years, the applications of induction machines in speed and position controlled drives have grown significantly. To achieve high efficiency and constant torque, many induction machines are constructed by attaching electronic control and they are used as speed and torque controlled drives. To achieve good static and dynamic characteristics of these drives, the engineers require a lot of information about the controlled machine. Thus, the parameter determination of the induction machine has become of first importance for the successful design of the electronic control.

There are several ways to predict the parameters of the induction motor equivalent circuit. Some of them are purely experimental, and some of them use numerical field computations and the Finite Element Method [1,3]. As the numerical field computation by the Finite Element Method requires good extent of knowledge, it is important to use an effective and intuitive finite element package to extract the machine parameters. Such a package is FEMM v. 3.3 (Finite Element Method Magnetics), which is freely available over Internet [2].

In this paper an investigation is made of the possibilities for application of the Finite Element Method and FEMM 3.3 software package for determination of induction machine equivalent T-circuit parameters (Fig. 1). The investigation is directed towards determination and corroboration of some existing relations between the FEM numerical solution and the classical per-phase equivalent circuit of the induction machine.

The equivalent circuit parameters, with their values and variations at working state, are used at the design stage of the control circuitry for a typical induction machine. The object of the present investigation is the induction machine model $\mathrm{AO}-042/4$, having rated power $P_n = 90$ W, rated rotor speed $n_n = 1370$ rpm, rated current $I_n = 0.37/0.64$, rated voltage $U_n = 380 / 220$ V, for $Y/\Delta$ connection.

In accordance with the aims of the investigation, an experimental determination of the induction machine parameters is achieved, using suitable load and no-load tests. Numerical

models of the same tests of the induction machine are developed using the finite element program FEMM 3.3 [2, 3].

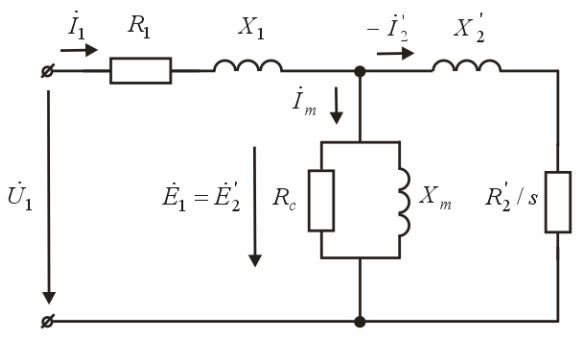


Fig. 1

## II. EXPERIMENTAL INVESTIGATION

In many cases the equivalent circuit of the induction motor is approximated by the traditional one shown on Fig. 1. In general, the parameters of this approximate circuit can be obtained by locked-rotor and no-load tests. In our case, the experimental investigation includes:

1) Locked-rotor test of the induction machine (slip $s = 1$), at which the characteristics $P_{1k}, I_{1k} = f(U_{1k})$ are determined. The interval of variation of the stator current is conforming to the requirements of the machine control.
2) No-load test (slip $s \approx 0$), at which the characteristics $P_{10}, I_{10} = f(U_{10})$ are determined.
3) Measuring the characteristics $P_1, I_1, n = f(M_2)$ in the interval $0 < s < s_m$ .
4) Measuring the resistance of the stator winding $R_{1t^0C}$ at the three cases above.

The results of the measurements are processed using the well-known analytical formulae:

A) From the locked-rotor test:

$$R_k = P_{1k} / 3I_{1k}^2;\ z_k = U_{1k} / I_{1k};\ X_k = \sqrt{z_k^2 - R_k^2} \tag{1}$$

The values of the stator winding reactance $X_1 = 54.21\,\Omega \approx const.$, the referred to the stator resistance of the rotor winding $R_2' = 101.03\,\Omega$ and the referred to the stator reactance of the rotor winding $X_2' = 50.36\,\Omega \approx const.$, which are parameters of the equivalent T-circuit, are found by solving the following algebraic system of equations:

$$\begin{cases} R_1 + R_2' = R_k \\ X_1 + X_2' = X_k \\ \dfrac{R_1}{R_2'} = \dfrac{X_1}{X_2'} \end{cases} \tag{2}$$

The last equation in the system (2) expresses an assumption, corroborated in many practical cases.

Because of the small height of the rotor slots of the machine under investigation - $h \approx 10\ mm$, the effect of current displacement in the locked-rotor test of induction machine (at frequency $f_2 = f_1 = 50$ Hz ) is negligible. Therefore, the current displacement coefficients $k_r$ for the resistance, and $k_x$ for the reactance, are equal to $k_r = k_x \approx 1$ in the whole range of rotor frequency variation $f_2 = s f_1$, for $1 \geq s > 0$. It can be expected that the value of $R_2'$, computed from the locked-rotor test, is a constant in the slip interval *s* shown above.

The computed values of the leakage inductances of the stator and rotor windings are $L_1 = X_1 / \omega_1 = 0.1726$ H and $L_2' = X_2' / \omega_1 = 0.1603$ H, where $\omega_1 = 2\pi f_1$. These parameters are practically constant, independent of the variations of currents $I_1$ and $I_2'$ at locked-rotor test, as well as in other working regimes. One of the reasons for that has been already shown above. The second reason consists in the fact, that by technological requirements, the width of the stator and rotor teeth of a small induction machine cannot be diminished much, which means that magnetic saturation does not occur at the specified currents.

B) From the no-load test:

For the correct functioning of the motor control system, the actual value of the mutual inductance $L_m$ is very important, as well as its variation. At the experimental approach, the mutual inductance is determined by the expression $L_m = X_m / \omega_1$, where the reactance of the magnetizing branch $X_m$ is found by solving the equation:

$$\dot{U}_{10} \approx j\dot{I}_{10}\left(X_1 + X_m\right) + \dot{I}_{10} R_1 \tag{3}$$

The obtained non-linear characterisic of the mutual inductance $L_m = f(I)$ is shown on Fig. 2.

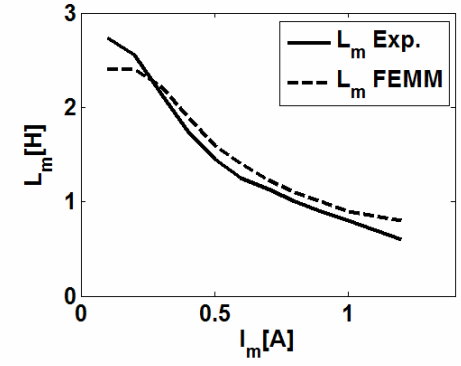


Fig. 2

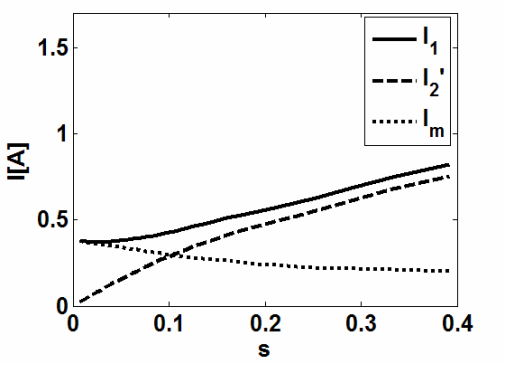


Fig. 3

## III. NUMERICAL SIMULATION

The numerical simulation of the induction machine under consideration is achieved by using the Finite Element Method and the software package FEMM 3.3 [2]. This package can solve "nonlinear time harmonic" electromagnetic problems using only the fundamental harmonic of the magnetic field intensity. The following nonlinear partial differential equation is solved:

$$\nabla \times \left( \frac{1}{\mu_{eff}(B)} \nabla \times \dot{A} \right) = -j\omega_s \sigma \dot{A} + \dot{J}_{src} - \sigma \nabla V \tag{4}$$

where: $\dot{J}_{src}$ - represents the phasor of the applied current source, $\dot{A}$ - is the phasor of the magnetic vector potential, $\mu_{eff}$ - is "effective permeability", $\sigma$ - is conductivity of the rotor slot material, $\omega_s$ is slip angular frequency.

The nonlinear time harmonic analysis includes the effects of nonlinearities like saturation and hysteresis on the fundamental of the response, while ignoring higher harmonic content. To model nonlinear eddy current problems using steady state analysis and phasors, it is necessary to use an "effective reluctivity" $\nu_{eff}(B) = 1/\mu_{eff}(B)$, which is independent of time. The effective reluctivity is defined by imposing the equivalence of the magnetic energy stored in the *BH* curve for the original magnetic field with higher harmonics and the effective *BH* curve associated with sinusoidally varying magnetic field. FEMM derives the effective *BH* curve by taking *H* to be a sinusoidally varying quantity. The amplitude of *B* is obtained by taking the first coefficient in a Fourier series representation of the resulting *B*.

The numerical simulation is done at specified stator current $\dot{I}_1$ and corresponding slip *s*, where the angular frequency $\omega_s$ in (4) is the slip angular frequency $\omega_s = s\omega$.

Because of the complicated geometry of the model and in order to facilitate the work with FEMM, the IMPAS CAD system [4] for design verification of induction machines was used. IMPAS acts as a GUI shell of FEMM, which automates the creation of the FE model by specifying only some of the typical machine parameters.

### 3.1 Mutual inductance $L_m = f(I)$

The numerical approach for determining $L_m$ is as follows. It is seen from Fig. 1, that

$$X_m = \frac{|\dot{E}_1|}{|\dot{I}_m|}; \text{ and thus, } L_m = \frac{X_m}{\omega_1} \tag{5}$$

This formula is correct when the iron losses are neglected ( $R_C \to \infty$ ).

#### 3.1.1 Determination the induced phase voltage from the numerical solution in FEMM

According to the theory of electric machines the induced voltage in the stator winding $\dot{E}_1$ can be determined by the formula

$$E_1 = \frac{\omega_1 u_k p \Phi_e}{a} = \omega_1 u_k' \Phi_F \tag{6}$$

where: $u_k$ - is the number of conductors in a stator slot; $u_k' = u_k / a$, where $a$ is the number of parallel branches of the winding; $p$ – is the number of pole pairs; $\Phi_e$ - is the embraced by a section group main magnetic flux; $\Phi_F$ - is the embraced by a whole phase main magnetic flux. Equation (6) is valid for both single- and double-layer windings. For the machine under investigation $u_k = 256;\ p = 2;\ a = 1$.

According to the expression of magnetic flux defined by a contour integral of the magnetic vector potential, $\Phi = \oint_{(\Gamma)} \mathbf{A}.\mathbf{dl}$, and taking into consideration the peculiarities of the stator winding with *q* sections in a section group, the magnetic flux $\Phi_e$ at core length $l_e$ can be found as:

$$\Phi_e = l_e \left\{ \sum_{i=1}^{q} \left[ \left| A_{(+)i} \right| + \left| A_{(-)i} \right| \right] \right\} \tag{7}$$

It is important that (7) is valid for fractional-pitch windings and also for distributed windings.

From the magnetic field distribution over the winding, the magnetic flux for a whole phase can be determined:

$$\Phi_F = p\Phi_e = l_e \left\{ \sum_{i=1}^{pq} \left[ \left| A_{(+)i} \right| + \left| A_{(-)i} \right| \right] \right\} \tag{8}$$

In (7) and (8), $A_{(\pm)i}$ denotes the average value of the magnetic vector potential $\dot{A}$ over the *i*-th section side with volume $V_{si}$.

$$A_{(\pm)i} = \frac{\iiint_{V_{si(\pm)}} A dV}{V_{si(\pm)}} \tag{9}$$

The numerator and the denominator in (9) are obtained by the FEMM's postprocessor. To find the induced voltage $E_1$, the necessary products for (7) and (8) can be computed as

$$l_e A_{(\pm)i} = \frac{\iiint_{V_{si(\pm)}} A dV}{S_{si(\pm)}} \tag{10}$$

where $S_{si}$ is the cross section of *i*-th section side.

### 3.1.2 Determination of the magnetizing current $I_m$ from the numerical solution in FEMM

According to the numerical algorithm of FEMM the stator winding currents and the induced rotor currents are sinusoidal variables in time that are represented in phasor notation as $\dot{I}_{s1(n)}$ and $\dot{I}_{s2(m)}$. The former is specified as input data, and the later is obtained from the solution of the quasi-stationary problem in FEMM. The indexes 1,2 correspond to the stator and rotor.

The magnetizing current $I_m$ is found by using the Ampere's circuital law and the expression for the magnetomotive force (*mmf*) in the induction machine:

$$\mathbf{F}_m = \mathbf{F}_1 + \mathbf{F}_2 \tag{11}$$

According to the electrical machines theory, the components of the *mmf* over the coordinates *x* and *y*, for the stator and the rotor, will be:

$$\begin{aligned} F_{1x} &= \sum_{n=1}^{Z_1} \mathrm{Re}\left[\dot{I}_{s1(n)}\right]\cos\left(p\alpha_{Z1(n)}\right) \\ F_{1y} &= \sum_{n=1}^{Z_1} \mathrm{Re}\left[\dot{I}_{s1(n)}\right]\sin\left(p\alpha_{Z1(n)}\right) \\ F_{2x} &= \sum_{m=1}^{Z_2} \mathrm{Re}\left[\dot{I}_{s2(m)}\right]\cos\left(p\alpha_{Z2(m)}\right) \\ F_{2y} &= \sum_{m=1}^{Z_2} \mathrm{Re}\left[\dot{I}_{s2(m)}\right]\sin\left(p\alpha_{Z2(m)}\right) \end{aligned} \tag{12}$$

Here, $\alpha_{Z1,2} = 2\pi / Z_{1,2}$ - is the geometrical angle between stator slots or between rotor slots ($Z_1$ and $Z_2$ are the numbers of stator and rotor slots). Since all quantities in (12) are known, the magnetizing current $I_m$ and the referred to the stator rotor current $I_2'$ can be determined. In this case both currents are referred to the stator winding:

$$I_m = \frac{\sqrt{F_{mx}{}^2 + F_{my}{}^2}}{K_{I_1}}; \quad I_2' = \frac{\sqrt{F_{2x}{}^2 + F_{2y}{}^2}}{K_{I_1}} \tag{13}$$

where

$$K_{I_1} = \frac{\sqrt{F_{1x}{}^2 + F_{1y}{}^2}}{I_1} \tag{14}$$

Evidently, if a referring to the rotor winding is necessary, the referring coefficient will be:

$$K_{I_2} = \frac{\sqrt{F_{2x}{}^2 + F_{2y}{}^2}}{I_2}$$

On Fig. 3 the computed values of the currents are shown, and on Fig. 4 – the phase differences between them for the regime under load according to point 3 of the experimental

investigations $/0 < s < s_m/$. The nearly linear increase of the phase difference between the magnetizing current $I_m$ and the referred rotor current $I_2'$ is fully in agreement with the interpretation of the equivalent circuit – Fig. 1. It can be seen that at low slip values this phase angle $\psi = arctg\left(s\,R_2'/X_2'\right) \approx s\,R_2'/X_2'$ is a linear function of the slip, and moreover, as it was shown before, $R_2'$ and $X_2'$ are constants in the range considered.

On Fig. 5 the phase differences between the currents at $s = 1$ are shown. It can be seen that the primary and the secondary currents at locked rotor test are nearly in opposite phase, which corroborates the main working hypothesis in investigating this regime.

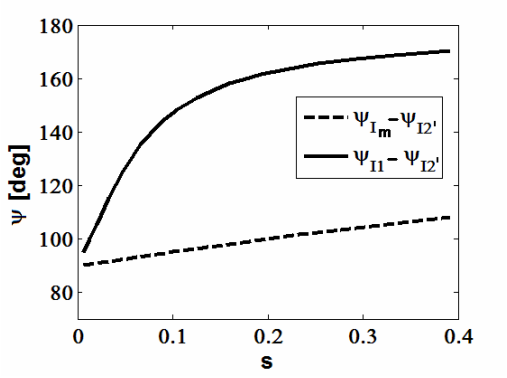


Fig. 4

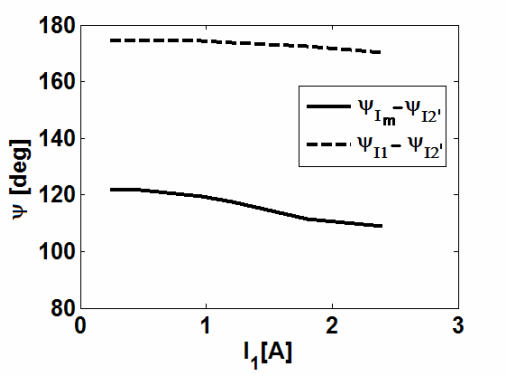


Fig. 5

After substitution of the numerical results for $E_1$ and $I_m$ in (5), the value of the mutual inductance $L_m$ is found. As $L_m$ is obtained by using the value of the induced voltage, on all figures it is denoted as $L_m(E)$.

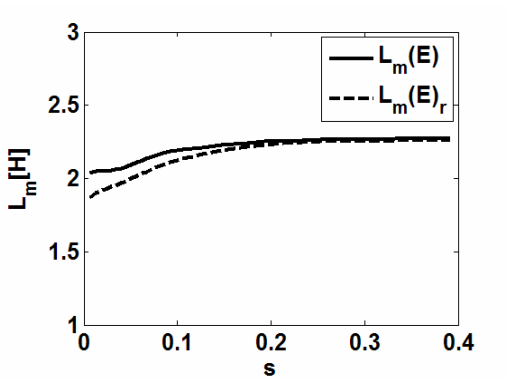


Fig. 6

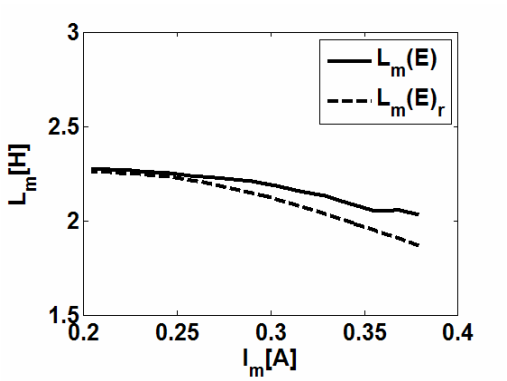


Fig. 7

The theory of transformers and induction machines states that the magnetizing current is the current, which creates the resultant magnetic flux of the machine when flowing through the stator winding at every working regime. In particular, the magnetizing current is considered as the current flowing through the stator winding at ideal no-load regime $/s = 0,\ I_2 = 0/$. This

formulation is checked and corroborated by creating numerical models with FEMM, where the stator winding is fed with the obtained values of the magnetizing current at $s = 0$, i.e., the load regime is "reduced" (concerning the magnetic state) to the ideal no-load regime. The difference in inductance values, computed for the two regimes, is used as a conformity criterion. In the reduced regime the inductance is denoted as $L_m(E)_r$.

The results from the numerical investigation are shown on Figs. 6 and 7. The biggest deviation between $L_m(E)$ and $L_m(E)_r$ does not exceed 8.5%.

As it has been already shown, at no-load regime, when neglecting the core losses $/R_C \to \infty/$, the no-load current is $I_{10} \equiv I_m$. In this case, the mutual inductance $L_m$ can be computed as [2]:

$$L_m(A.j) = \frac{\iiint_{V_\Sigma} A.jdV}{I_{m(\pm)}^{\ 2}} \tag{15}$$

where: $I_{m(+)} = -I_{m(-)}$ and with correspondence with its physical meaning $\left|\dot{I}_m\right| = \left|\dot{I}_{m(\pm)}\right| = I_m$.

If the following formulae are taken into account:

$V_\Sigma = V_{s1} + V_{s2} + \cdots + V_{spq}$; $\quad V_{s1} = V_{s2} = \cdots = V_{spq} = V_s$; $\quad j_{(\pm)} = \frac{I_{m(\pm)} u_k}{a S_s}$; $\quad S_s = \frac{V_s}{l_e}$; then, after substitution and transformations in (15) the following expression is obtained:

$$L_m(A.j) = \frac{u'_k\, l_e}{V_s}\left\{\sum_{i=1}^{pq}\left[\frac{\iiint_{V_{si(+)}} AdV}{I_{m(+)}} + \frac{\iiint_{V_{si(-)}} AdV}{I_{m(-)}}\right]\right\} \tag{16}$$

But, if $\iiint_{V_{si(+)}} AdV > 0$, then $\iiint_{V_{si(-)}} AdV < 0$, $\frac{\iiint_{V_{si(+)}} AdV}{I_{m(+)}} > 0$ and $\frac{\iiint_{V_{si(-)}} AdV}{I_{m(-)}} > 0$.

Therefore, equation (16) can be expressed as

$$L_m(A.j) = \frac{u'_k\, l_e}{I_m}\left\{\sum_{i=1}^{pq}\left[\left|\frac{\iiint_{V_{si(+)}} AdV}{V_s}\right| + \left|\frac{\iiint_{V_{si(-)}} AdV}{V_s}\right|\right]\right\} \tag{17}$$

This expression is identical to the expression for $L_m(E)$, that would be obtained if all quantities defined by formulae (6)÷(10) are substituted in (5). The confirmation of this can be seen on Fig. 8. The difference between $L_m(E)$ and $L_m(A.j)$ does not exceed 4 %.

### 3.2 Leakage inductance of the stator winding $L_1 = f(I)$

As it was shown in Section II, the leakage inductance for the induction machine is practically constant. For its numerical determination the same algorithm is used as before in calculating $L_m$ at two types of models:

(i) With rotor at $s = 1$;

(ii) Without rotor.

The investigations are made at the same current in the stator winding as those applied in the experiment. The results are shown on Fig. 9. The comparison with the experimental data shows, that the second model is more suitable for determination of the leakage inductance, especially as the numerically found leakage inductance is only for the slot part of the winding.

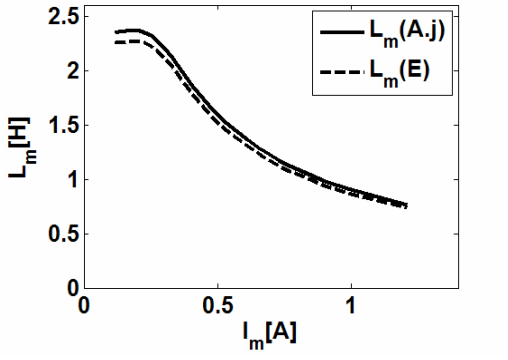


Fig. 8

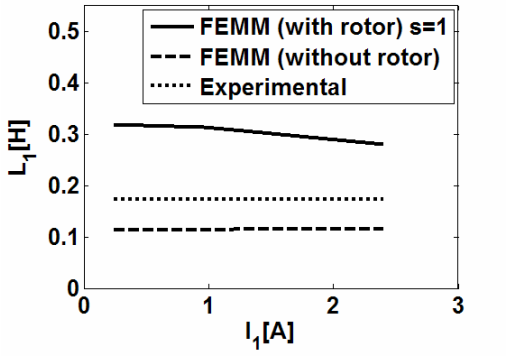


Fig. 9

### 3.3 Rotor resistance of the induction machine

The numerical solution produced by FEMM contains the value of the electrical losses $P_{el2}(s)$ in the slot part of the rotor winding for every value of the slip *s*. This gives the following opportunities:

- Using the already determined value of the referred rotor current (13), the referred rotor resistance $R'_{2s}$ *of the rotor winding slot part* can be computed:

$$R'_{2s}(s) = \frac{P_{el2}(s)}{3I'_2(s)} \tag{18}$$

- The current displacement coefficient $k_r = f(s)$ of the rotor winding slot part can be determined (accounting for the rotor bar skin effect):

$$k_r = \frac{R'_{2s}(s)}{R'_{2s}(s \le s_n)} \tag{19}$$

The inequality $s \le s_n$ shows that in the denominator of (19) the value of $R'_{2s}$ at sufficiently small slip value must be used.

- Using the expression $R'_{2s} = K_I K_U R_{2s}$, the coefficient $K_U$ can be determined:

$$K_U = \frac{R'_{2s}}{K_I R_{2s}} \tag{20}$$

The function of the computed resistance $R'_{2s}$ with respect to the slip *s* is shown on Fig. 10.

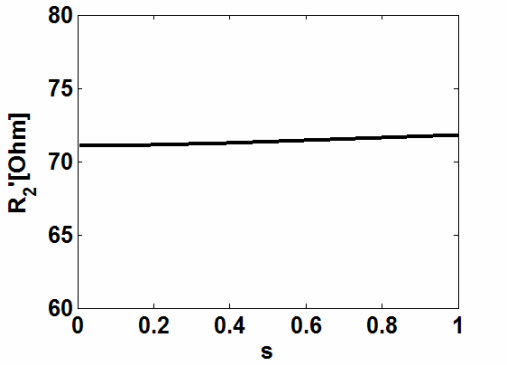


Fig. 10

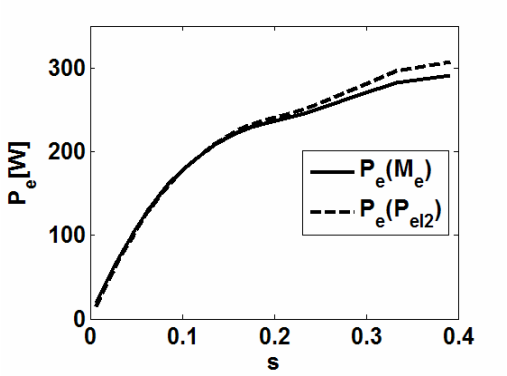


Fig. 11

### 3.4 Electromagnetic power and torque of the induction machine

It is known, that using the equivalent electric T-circuit, the electromagnetic power of the induction machine can be given as:

$$P_{\delta(p_{el2})} = \frac{P_{el2}(s)}{s} \tag{21}$$

From the FEMM solution, the electromagnetic torque of the machine $M_{\delta FEMM}(s)$ can be found. It can be also used for determination of the electromagnetic power:

$$P_{\delta(M_\delta)} = M_{\delta FEMM}(s)\frac{\omega_1}{p} \tag{22}$$

On Fig. 11 the electromagnetic power determined using both approaches is shown. The absolute value of the difference does not exceed 5 %.

On Fig. 12 the graph of the function of the experimentally obtained torque $M_2(s)$ and the graph of the torque $M_{2FEMM}$ found by FEMM (additionally corrected with the torque corresponding to the experimental mechanical losses), are displayed. In order to find the computed torque curve, a corrected rotor conductivity has been utilized corresponding to the rotor temperature, and a certain increase of the slot active resistance has been introduced, to account for the end-windings resistance.

During the investigation of the electromagnetic power and torque, it was found that at rotor slot numbers $Z_2 = Z_1/2$ or $Z_2 = Z_1$, the discrepancy between $P_{\delta(p_{el2})}$ and $P_{\delta(M_\delta)}$ becomes higher than 160 %. The investigation has been conducted at the condition, that the

sum of rotor slot areas is maintained approximately constant. It is seen from Fig. 13, that at these values of $Z_2$ the electromagnetic torque strongly decreases. Evidently, there exists some reactive synchronous torque in the case of $Z_2 = Z_1 / 2$ or $Z_2 = Z_1$. Also, it is known, that on these reasons (the appearance of synchronous reactive torques at start), the shown ratios between the stator and rotor slot numbers are forbidden for the design practice. Therefore, from one side, the found discrepancy confirms the theory, and from another side – it can be used as indicator of appearance of similar adverse phenomena.

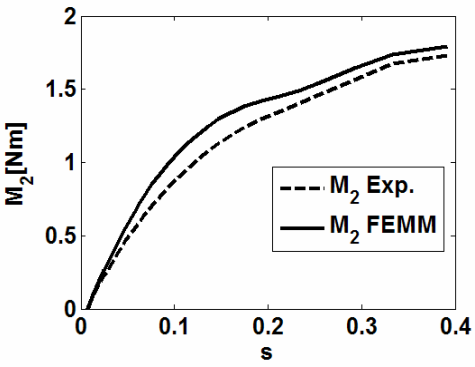


Fig. 12

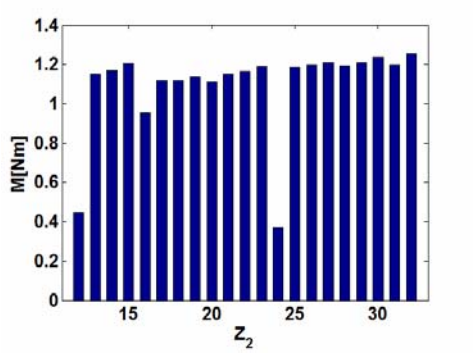


Fig. 13

## IV. CONCLUSIONS

The analysis of the numerical results obtained with FEMM 3.3 software and their comparison with the experimental data leads to the following conclusions:

- The mutual inductance $L_m$ has been found by two approaches – by numerical analysis of the model under load, and by numerical analysis of the simulated ideal no-load regime. The difference found is due to the non-sufficiently accurate representation of the spatial distribution of the magnetizing current in the model at ideal no-load test, because of the discrete distribution of the stator winding.

- The mutual inductance $L_m$ is a parameter not related to the end-windings of the machine and thus the end-effects do not influence its value. Therefore, the 2D analysis does not diminish the accuracy of $L_m$ computation. In a larger part of the investigated function /Fig. 2/, the computed values of $L_m$ are higher than the experimental ones. The reasons for this can be the processing of the experimental data, and also the fact, that the leakage inductance of the slot part is included in the computation of $L_m$. The later drawback can be excluded, as FEMM computes $L_m$ with sufficient accuracy.

- The 2D analysis influences the accuracy of computed rotor winding parameters, as the end-windings are not taken into account. However, this adverse effect is diminished considerably at higher ratio of active core length to pole pitch length.

- The 2D analysis can be used successfully in the study of the parameters and the phenomena related to the slot part of the rotor bars, for the current displacement coefficient $k_r$, and for the reactive torques appearing at special ratios in the geometry of the rotor and stator cores.

The obtained equivalent circuit parameters have been already successfully used as basic values in the design of vector control circuitry of the induction machine under investigation.

**References:**

[1] Zhou P., J. Gilmore, Z. Badics, Z. Cendes, Finite Element Analysis of Induction Motors Based on Computing Deatailed Equivalent Circuit Parameters, IEEE Trans. Magnetics, vol. 34, No. 5, Sept. 1998, pp. 3499-3502.
[2] Meeker D., Finite Element Method Magnetics v. 3.3 User's Manual, August 17, 2003.
[3] Meeker D., Induction Motor Example, dmeeker@ieee.org, September 26, 2002
[4] Mihaylova P., K. Brandisky, M. Mihov, CAD System For Performance Prediction Of Induction Motor Using The Finite Element Method, 7th International Conference On Applied Electromagnetics PES 2005, Nish, Serbia & Montenegro, 23 - 25 May 2005.

**Authors:**

Assoc. Prof. Dr. Miho Mihov
Assoc. Prof. Dr. Kostadin Brandisky
Assoc. Prof. Dr. Emil Ratz
Eng. Pavlina Mihaylova
Technical University of Sofia
8, Kliment Ohridski Blvd., 1000 Sofia, Bulgaria
Phone: +359-2-965-3809
E-mail: mpmi@tu-sofia.bg kbran@tu-sofia.bg